

Anisotropic properties identification of Naintupo Formation, Tabul Formation and Tarakan Formation (Tarakan Sub-Basin) using anisotropic parameters determination method from P- wave seismic diffraction

Submission date: 05-Sep-2024 07:26AM (UTC+0700)

Submission ID: 2434701352

File name: on,_Tabul_Formation_and_Tarakan_Formation_Tarakan_Sub-basin.pdf (596.66K)

Word count: 3667

Character count: 18878

by Imam Setiaji Ronoatmojo

PAPER · OPEN ACCESS**Anisotropic properties identification of Naintupo Formation, Tabul Formation and Tarakan Formation (Tarakan Sub-Basin) using anisotropic parameters determination method from P-wave seismic diffraction function**

To cite this article: I S Ronoatmojo and M Burhannuddinur 2018 *IOP Conf. Ser.: Earth Environ. Sci.* **212** 012075

View the [article online](#) for updates and enhancements.

Anisotropic properties identification of Naintupo Formation, Tabul Formation and Tarakan Formation (Tarakan Sub-Basin) using anisotropic parameters determination method from P-wave seismic diffraction function

I S Ronoatmojo^{1*} and M Burhannudinnur¹

¹Faculty of Earth Technology and Energy, Trisakti University, Campus A, Building D, 2nd Floor, Jl. Kyai Tapa No.1, Grogol, Jakarta 11440, Indonesia.

*corresponding author: aji.rono@trisakti.ac.id

Abstract. The anisotropic property of sedimentary rocks are influenced by geological processes such as sedimentation pattern, grain size and grain sorting, hence it might be a significant impact to the seismic wave propagation. An identifying method of the anisotropic property is done by deriving the relationship between group velocity and phase velocity of a P-wave seismic diffraction function. Subject to be studied are Naintupo Formation, Tabul Formation and Tarakan Formation which are lied in Tarakan Basin, these formations are an anisotropic sedimentation products, generally composed of sandstone and shalestone by thickness more than 1000 meters. In the seismic section, it is shown by range of 1500 msec - 3000 msec. The diffraction function observed at a point of the diffractor due to the normal fault. There are 3 points of observation, SP.1374, SP.1375 and SP.1376 which assign anisotropic value δ and ϵ , where the δ value is in the range of 0.26 – 0.28 and the ϵ value is in the range of 0.46 – 0.72, picked from 42 samples. Furthermore, Pre Stack Depth Migration was carried out through 2 velocity models; there are velocity model with anisotropic parameters δ and ϵ derived from diffraction functions and the constrained velocity inversion method. After the curved ray pre-stack migration process, it is found that the velocity $V_p(90^\circ)$ of diffraction method faster than the constrained velocity inversion method, where the δ value for both methods are 0.35 but the ϵ for the diffraction method is 0.4 and the constrained velocity inversion method is 0.35. Regarding to the result of the 2D NW-SE PSDM stack, there is a more obvious fault compartment observed from the diffraction method.

Keywords: sedimentation, anisotropic parameters, diffraction.

1. Introduction

Naintupo Formation, Tabul Formation and Tarakan Formation are sedimentation products lied in the Tarakan Basin. Tarakan Basin itself subdivided into Tidung Sub-basin, Berau Sub-basin, Tarakan Sub-basin and Muara Sub-basin, however the boundaries between the sub-basins are not always effective borders, some are only hinges or fault zones. The basin subsidence developed and opened to the east and the sea transgressed westward, and marine shale of Sembakung Formation were deposited overlying the Dannu basement rocks. The latest Eocene uplift interrupted the transgression which produced Sujau Formation (coarse clastic), a carbonate platform of Seilor Formation and continued became Mangkabua



Content from this work may be used under the terms of the [Creative Commons Attribution 3.0 licence](https://creativecommons.org/licenses/by/3.0/). Any further distribution of this work must maintain attribution to the author(s) and the title of the work, journal citation and DOI.

Shales. The western basin margins were uplifted and caused open marine condition to widespread and rapid clastic deltaic deposition, which prograded eastwards in the Middle Miocene [1]. In this period time, the sedimentation process generated the thick sand-shale lithology with anisotropic tendency consist of Naintupo Formation, Tabul Formation and Tarakan Formation.

The sedimentation process during this period was influenced by the regular NE-SW trending faults which are normal to the sedimentary thickening direction, it seems direct result of successive deltaic sediments loading [1]. The anisotropic property can be described as an orientation of the deposition pattern which is controlled by tectonic activities through this period. Lithology fabric and pore geometry are important factors in the velocity of wave propagating through medium. The characteristic of the anisotropic rock is reflected from the velocities measured are not similar in different directions. Substantially, this is caused by the effect of preferred alignments of geological components. For example, at the pore scale, shale prone rocks are anisotropic owing to the alignment of clay minerals. Anisotropic effects can also occur at the seismic scale owing to sedimentary layering and vertical fracturing [2]. Moreover, these effects relating with pore geometry and rock fabric on elastic properties. These bounds are a useful type of rock physics model, essentially representing different ways of mixing rock and fluid; the softest possible mix is the Reuss bound (harmonic average) and the stiffest is the Voigt bound (arithmetic average). It is evident from figure 1 that the Reuss bound effectively describes the behaviour of suspensions. Note that the yellow points refer to marine ooze data acquired at or close to the seabed. The sand-shale intercalation which is the mixing situation between suspension sedimentary process tend to have Reuss bound with a Voigt-Reuss bound. The Reuss bound itself reflects the flattened clay minerals due to suspension and compaction. The intensity of this process can be illustrated from this figure as the sand-shale porosity and velocity discrimination, belong to the change of pore geometry and rock fabric [2].

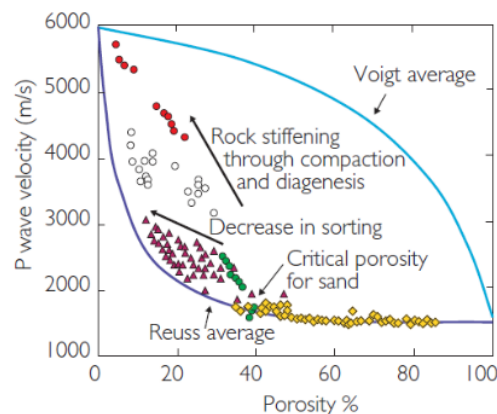


Figure 1. Velocity-porosity characteristics of brine bearing siliciclastic sediment [2].

In term of our study, anisotropic property related to layering. The aligned particles in shale units as well arranged layers horizontally on smaller scale than the seismic wavelength. For this anisotropic property type varies with incidence angle where horizontal layer velocity is faster than vertical velocity but within a plane perpendicular to the symmetry axis, it does not show any variation with direction. As this layering conforms to polar symmetry, the anisotropy that results from this type of configuration is referred to polar anisotropy. It is also commonly called *vertical transverse isotropy* or VTI that plane perpendicular to the symmetry axis is essentially isotropic [3].

The real impact of anisotropic problem is flattening reflector. It occurs when the reflector in a gather is difficult to be flatten beyond an incidence angle of about 30° with standard moveout corrections. It is

pointed out the effect of *vertical transverse isotropy* (VTI) on the seismic travel time for a VTI medium [4] then the travel time can be described by:

$$T_x^2 = T_0^2 + \frac{x^2}{V_{NMO}^2} - \frac{2\eta x^4}{V_{NMO}^2 (T_0^2 V_{NMO}^2 + (1+2\eta)x^2)} \quad (1)$$

where η is given by Thomsen's parameter:

$$\eta = \frac{\varepsilon - \delta}{1 + 2\delta} \quad (2)$$

and,

$$V_{NMO} = V_{P0} \sqrt{1 + 2\delta} \quad (3)$$

while V_{P0} is the P-wave vertical velocity.

The η parameter is usually derived from stack semblance optimization after initial velocity estimation in time processing [5]. A combination of time migration and depth migration can provide the information on anisotropic parameters δ and ε , which δ can be estimated iteratively from the misties between a depth migrated image and the true depth as measured from well data, and then ε can be estimated from the combination of η and δ [6].

The VTI anisotropic tendency occurs in the far offset. It is identified from the remain of normal move out correction such as described in equation (1). Therefore, the anisotropic tendency commenced to be observed after the late of 1980's when the far offset arise to be used in the seismic survey. The real impact of the anisotropic tendency in the seismic data processing is the ability of NMO data correction flattening, which is anisotropy appeared in the unflattened data correction. The NMO data correction accuracy may have an impact in the seismic imaging result, both for PSTM (pre-stack time migration) and PSDM (pre-stack depth migration).

2. Methodology

The 2D NW-SE seismic data which is used for this study was conducted in the Macassar Strait along 27.2 km's (2041 point CDP's) in 1991. Generally, the data quality is fair to good which is static correction problem not found due to the survey conducted in offshore, however the seismic data is somewhat disturbed by the multiple reflectors caused by the high contrast of impedance. Despite of the 1991 data, the signal to noise ratio is high as a consequence of the multiple coverage is 73%. The streamer length which was used up to 4 km's, so it has a far offset value causing anisotropic effect. Based on the acquisition parameters statistics, it is observed that the receiver array is a 4000 m length generating an offsets distribution which is dominated by offset range 1200 m - 1500 m, 2400 m - 2700 m and 3600 m - 3900 m. Beside of it caused anisotropic effects, these also generate multiple which is appeared in the range of 1800 msec to 3400 msec. Meanwhile, the seismic wave in the fault plane diffracted along Sujau Formation. Furthermore, the equation which transforms to the diffraction based on geometry such as shown in figure 2 [7].

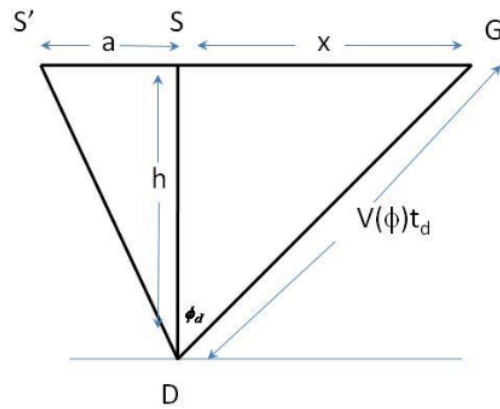


Figure 2. Diffraction geometry [7].

Referring to the diffraction geometry and the assumption of $\tan\theta = \tan\phi$, then if $Z = \sin^2\theta$ [7]:

$$Z = \left[\frac{\tan^2\phi}{1 + \tan^2\phi} \right] \tag{4}$$

or,

$$x^2 = \left[\frac{Zh^2}{(1-Z)} \right] \tag{5}$$

where h is the thickness of medium. If the the diffraction travel time is the source to receiver offset function which is expressed as t_x , then:

$$t_x = t_k + t_d \tag{6}$$

In this case t_k is the diffraction delay time or the travel time along the S'D segment when the source is in the distance a from a diffractor projection point in the surface, then t_k will change to $\frac{t_0}{2}$ if $a = 0$, or the source is above the diffractor point. It appears from the relationship in the right triangle S'SD that the t_k is

$$t_k = \frac{t_0\sqrt{a^2 + h^2}}{2h} \tag{7}$$

and,

$$\frac{t_0}{2} = \frac{t_0'}{\left(\frac{\sqrt{a^2 + h^2}}{h} + 1\right)} \quad (8)$$

Meanwhile, the polynomial equation used in this study is an equation which states the relationship between group velocity and phase velocity in determining anisotropic parameters [7][8].

$$V(\phi)^2 = V^2(0)(1 + (2\delta + 4\delta^2)Z + (2\eta + 16\delta\eta - 3\delta^2)Z^2 + (16\eta^2 - 14\delta\eta)Z^3 - 15\eta^2Z^4) \quad (9)$$

where $z = \sin^2\theta$.

The equation can be written to be:

$$V(\phi)^2 = V^2(0)(1 + pZ + qZ^2 + rZ^3 + sZ^4) \quad (10)$$

with p, q, r and s replacing the coefficients of polynomial order. Then if equation (7) and equation (8) is substituted to equation (10), the equation will become:

$$\left(\frac{h^2}{(1-Z)}\right) = t_0'^2 V^2(0)(1 + pZ + qZ^2 + rZ^3 + sZ^4) \quad (11)$$

The anisotropic parameters will be calculated by above method then the result of each methods (diffraction and CVI) will be applied to the depth migration process before stack. The work-flow of depth migration processing before stack as shown in figure 3. It is started from inputting several gathers as result of pre-stack time migration. Then, after interval velocity calculation to obtain the initial model, tomography process was done to get the velocity model based on the ray-path modeling. At that step, the result of anisotropic parameters estimation of 2 methods were inserted, through an iteration process to get a residual of each δ and ε which must be rectified to obtain an optimal CRP (Common Reflection Point) gathers which will be stacked.

3. Data and Discussion

Based on the 2D pre-stack time migration as shown in figure 4 that the diffraction effects appear as well in the fault plane along the anisotropic medium of Naintupo Formation, Tabul Formation and Tarakan Formation, the diffraction picked up on the fault plane that touch the Sujau Formation.

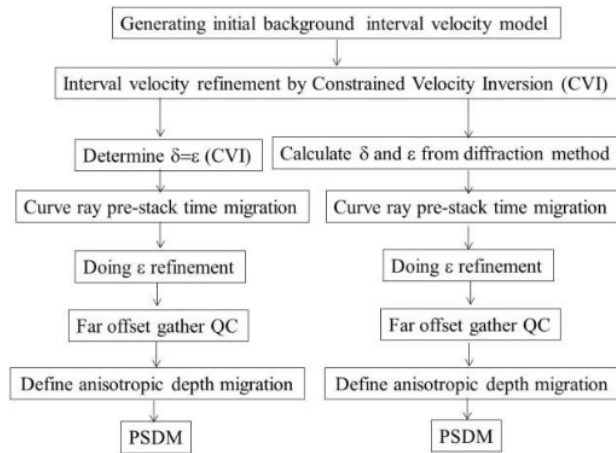


Figure 3. Work-flow of study.

There are at least 5 major faults as the main factor of deformation to the sedimentary product. It seems that the main fault develop in the northwest part of this section, which the area encircled by red line (figure 4). This fault plane can discontinue the seismic energy, consequently it becomes a scattered energy point. This energy will propagate as an diffracted seismic wave to all direction along the medium, therefore it can be observed from the difference between group velocity and phase velocity as the way to estimate the anisotropy parameters.

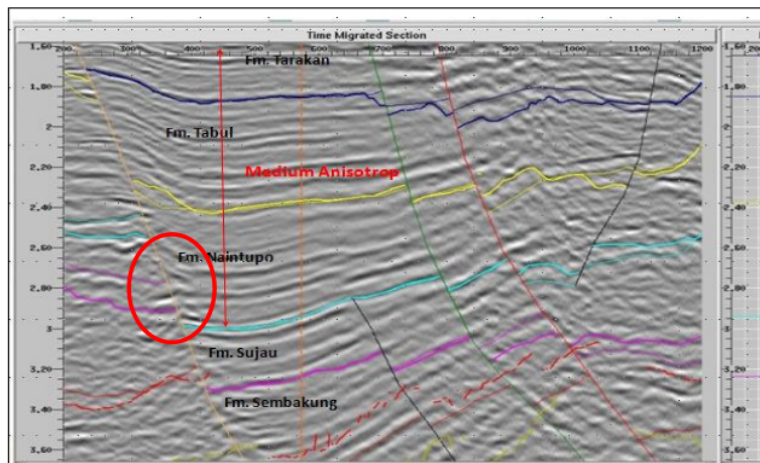


Figure 4. Pre-stack time migration section, diffraction effects can be observed in the encircled area by red line.

Meanwhile, regarding to the sedimentary progradation to the northwest, the sedimentary product will be thickening and strengthening the point of observation. Furthermore, as shown in figure 5 there are shotpoint gathers display of SP. 1374 - SP.1376, it is seen that the diffraction effect arise when a seismic wave beam reach fault plane around CDP.361 at a time range of 3000 msec to 3600 msec with the appearance of a hyperbolic function with a sharper slope of the reflection seismic function. Diffraction effect also appearing on CDP. 781 and CDP. 921 resulting from the existence of other fault planes. However, the choice of observation is around CDP.361, which is projected to the surface as SP.1374, SP.1375 and SP.1376 because diffracted P-wave propagating along the anisotropic medium in this position.

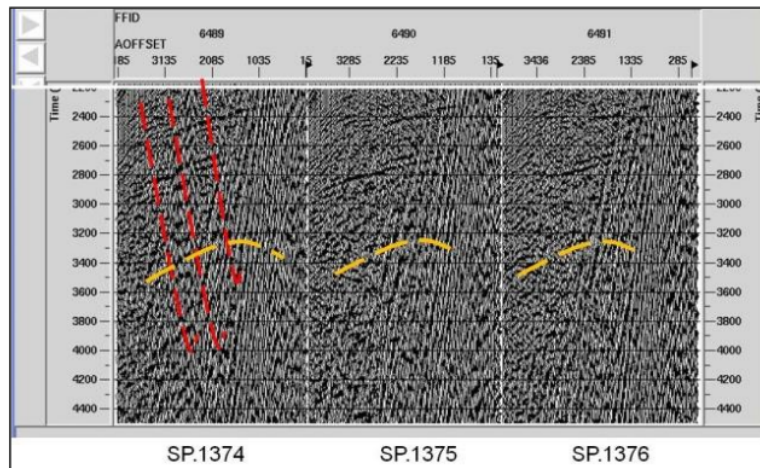


Figure 5. SP.1374 to SP.1376.

It is observed that the average values gained from SP.1374, and SP.1375 provide a consistent value of 0.28 with standard deviation is 0.0117 (SP.1374) and 0.0118 (SP.1375), while for SP.1376 the value of δ is 0.26 with standard deviation is 0.0119 (table 1). The average ϵ attained from SP.1374 is 0.46 with standard deviation is 0.0185, SP.1375 of 0.48 with standard deviation is 0.0174, and the value of slightly differed significantly in SP.1376 is 0.72 with standard deviation is 0.0015.

Velocity modeling is a forward and inversion modeling. The transformation process based on *ray tracing principle* after horizon picking interpretation. This processing is aimed to get interval velocity. There are 2 velocity models in this study which is built with an anisotropy parameters derived from diffraction function and constrained velocity inversion method. Then, δ and ϵ applied on the CRP domain. Furthermore, it can be acquired from the "semblance" of spectrum whether the velocity model is correct or not. An error will be appeared in the corrected common offset data as a non-flat layer on a CRP domain. This is not due to erroneous migration but the anisotropy effect on far offset (> 2000 m) in CRP domain.

Table 1. The anisotropy parameters calculated by diffraction method.

No.	CDP. 1374		CDP. 1375		CDP. 1376	
	δ	ϵ	δ	ϵ	δ	ϵ
1.	0.292	0.481	0.291	0.502	0.272	0.726
2.	0.291	0.480	0.290	0.501	0.271	0.726
3.	0.289	0.477	0.288	0.498	0.267	0.725
4.	0.287	0.474	0.286	0.495	0.266	0.724
5.	0.286	0.473	0.285	0.494	0.265	0.724
6.	0.285	0.471	0.284	0.492	0.264	0.724
7.	0.282	0.466	0.281	0.488	0.261	0.723
8.	0.279	0.460	0.278	0.482	0.257	0.723
9.	0.274	0.453	0.273	0.475	0.253	0.722
10.	0.270	0.447	0.269	0.469	0.249	0.722
11.	0.266	0.440	0.265	0.463	0.245	0.722
12.	0.262	0.433	0.261	0.457	0.241	0.722
13.	0.257	0.427	0.256	0.450	0.235	0.722
14.	0.252	0.417	0.251	0.443	0.231	0.723
Avg =	0.28	0.46	0.28	0.48	0.26	0.72
STDEV =	0.0117	0.0185	0.0118	0.0174	0.0119	0.0015

It can be mentioned that the anisotropic properties of medium will affect NMO correction, the horizontal velocity accuracy level expressed by the η or $(\epsilon-\delta)$ value [9]. The velocity analysis is obtained from "semblance" then the velocity value will be seen from "the power spectrum" value of single constant velocity, if the value is not optimal then the correction is only for the near offset. Therefore if η has not been entered, the accurate NMO velocity value for far offsets can not be achieved, consequently it will reduce the stack resolution. Similarly, if the η value is not correct as a consequence it can be known from δ residual and ϵ residual. However, each calculation has incorporated an anisotropy assumption but it will be tested to understand what extent the error occurring in each velocity model built on that anisotropic parameters value by viewing the residual value of δ and residual value of ϵ before the refinement process.

The result which is obtained after *the curved ray pre-stack migration process* appearing V_p (90°) of diffraction method (5500 m/sec - 6000 m/sec) is faster than the constrained velocity inversion method (5300 m/sec – 5800 m/sec). The δ value for the diffraction method and the constrained velocity inversion method are 0.35, while the ϵ for the diffraction method is 0.4 and constrained velocity inversion method is 0.35. The δ and ϵ values indicating how large the difference between group velocity and phase velocity which

will shift the reflector point as an impact of energy propagation along the anisotropic sedimentation product. The δ value relates to the vertical component and the ϵ value relate to horizontal component. So, the difference accuracy of both methods have been found in the ϵ determination, or in another word, the ϵ determination is the important factor and it is originate coming from the horizontal impact of anisotropy.

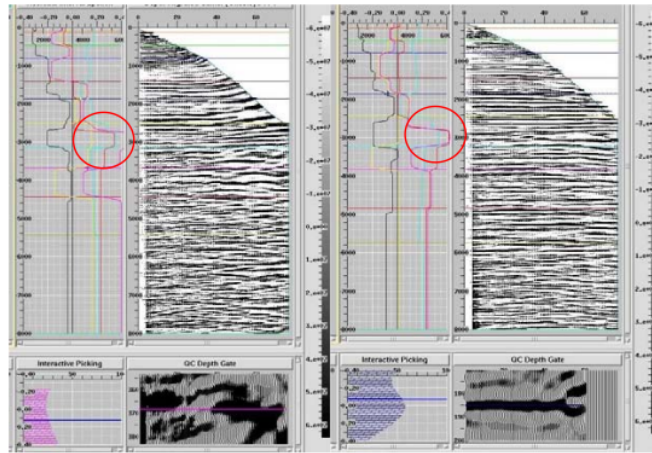


Figure 6. Residual ϵ for a) seismic method constrained velocity inversion and b) diffraction method on CDP. 750.

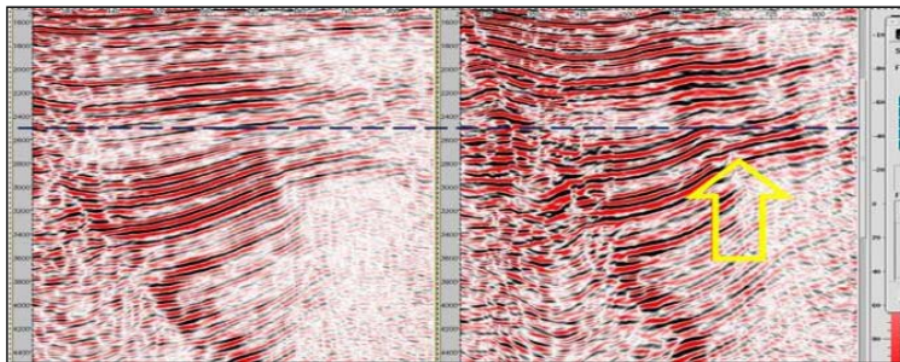


Figure 7. Migration cross-section before stack in depth domain a) with anisotropic parameters calculated from the constrained velocity inversion method, b) with the anisotropic parameters calculated from the diffraction method.

Figure 6 demonstrates in the ϵ residual observation that the reflector's appearance on the diffraction method is much better than the constrained velocity inversion method. This means that the ϵ refinement of CVI method is greater than diffraction method (approximately +0.05). This can be done as an alternative in cases where PSDM processing is performed in the area without well data. By observing the stack results qualitatively of each method it appeared that the horizon depth of the diffraction method is shallower than

CVI method, this may be caused by the horizontal velocity of diffraction method is faster than the result of the constrained velocity inversion method. There is also seen that a better image of curvature was found in the diffraction method at depth of 2500 msec as shown in figure 7.

4. Conclusions

The Naintupo Formation, Tabul Formation and Tarakan Formation were formed in the anisotropic environment with a vertical anisotropic tendency that can be observed through the diffracted P-wave seismic caused by fault plane that intersecting formations. The diffracted wave may give a better impact of the relationship between group velocity and phase velocity that can be used to determine how large a shifting position occurs due to the nature of anisotropy. In this study, the horizontal velocity obtained from the diffraction method (5500 m/sec – 6000 m/sec) is faster than the CVI method (5300 m/sec – 5800 m/sec) and it performing a smaller refinement correction after ray curve analysis (nearly -0.001).

Regarding to the observation result of the 2D NW-SE PSDM stack, there is a more obvious fault compartment observed on the diffraction method, where the NW part of fault throw offset is larger than the SE part of fault. This corresponds to the regional tectonic reconstruction which the rapture intensity increases toward to northwest.

Acknowledgments

The authors would like to thank the Ministry of Mineral and Energy Resources of Republic Indonesia and SKKMIGAS which has permitted to use data for these purposes. Also thank to PT. Elnusa Tbk which has provided their processing center to facilitate this research. By these results, hopefully we can able to enhance the capabilities and productivities.

11

References

- [1] Darman H and Sidi F H 2000 *An outline of the geology of Indonesia* (IAGI) p 75-77
- [2] Simm R and Bacon M 2014 *Seismic Amplitude: An Interpreter's Handbook* (Cambridge University Press) p 7-40 and p 69-70
- [3] Thomsen L 2002 *Understanding seismic anisotropy (Distinguished Instructor Short Course no 5 SEG/EAGE)* p 1-4
- [4] Alkhalifah T 1997 *Velocity analysis using nonhyperbolic moveout in transversely isotropic media (Geophysics 62)* p 1839-1854
- [5] Toldi J, Alkhalifah T, and Berthet P 1999 *Case study of estimation of anisotropy (The Leading Edge 18)* p 588-594
- [6] Jones I F 2010 *An Introduction to Velocity Model Building* (Houten: EAGE Publications) p 50-56
- [7] Ronoatmojo I S, Santoso D, Sanny T A and Fatkhan 2011 *Pendekatan polinomial orde-3 hubungan kecepatan grup dan fase dalam estimasi tetapan anisotropi medium isotrop transversal tegak dari difraksi gelombang seismik-P (Jurnal Geofisika No.1 Th. 2011)* p 11-24
- [8] Helbig K and Thomsen L 2005 *75-plus years of anisotropy in exploration and reservoir seismic (Geophysics 70)* p 9-23
- [9] Alkhalifah T and Tsvankin I 1995 *Velocity analysis for transversely isotropic media (Geophysics, 60)* p 1550-1566

Anisotropic properties identification of Naintupo Formation, Tabul Formation and Tarakan Formation (Tarakan Sub-Basin) using anisotropic parameters determination method from P-wave seismic diffraction

ORIGINALITY REPORT

16%

SIMILARITY INDEX

14%

INTERNET SOURCES

11%

PUBLICATIONS

5%

STUDENT PAPERS

PRIMARY SOURCES

1	speakerdeck.com Internet Source	4%
2	ejournal.undip.ac.id Internet Source	2%
3	Submitted to Universitas Negeri Surabaya The State University of Surabaya Student Paper	1%
4	www.asx.com.au Internet Source	1%
5	www.scribd.com Internet Source	1%
6	www.hagi.or.id Internet Source	1%
7	simakip.uhamka.ac.id Internet Source	1%
8	Submitted to uu Student Paper	1%

9	www3.ogs.trieste.it Internet Source	1 %
10	csegrecorder.com Internet Source	<1 %
11	R Adikusuma, D N Sahdarani, F M H Sihombing, Supriyanto, G T M Kadja. "Petrology and petrogenesis of igneous rock in Mount Endut, Banten Province", IOP Conference Series: Earth and Environmental Science, 2020 Publication	<1 %
12	Submitted to University of Baghdad -College of Mass Communication Student Paper	<1 %
13	multisitestaticcontent.uts.edu.au Internet Source	<1 %
14	Imam Setiaji Ronoatmojo, Muhammad Burhannudinnur, Grace Stephanie Titaley. "The effect of effective stress on pore pressure and velocity relationship in tectonic mechanism", AIP Publishing, 2023 Publication	<1 %
15	Submitted to University of Witwatersrand Student Paper	<1 %
16	cdn2.hubspot.net Internet Source	<1 %

17 HAO, Chong-Tao, and Chen YAO. "Analytic Approximation of Quartic Moveout Coefficient in the TI Media with an Arbitrary Spatial Orientation", Chinese Journal of Geophysics, 2009.

Publication

<1 %

18 e-journal.trisakti.ac.id

Internet Source

<1 %

19 repository.unusa.ac.id

Internet Source

<1 %

20 umpir.ump.edu.my

Internet Source

<1 %

21 www.cambridge.org

Internet Source

<1 %

22 Geoffrey A. Abers. "Chapter 149 Subduction Zones", Springer Science and Business Media LLC, 2021

Publication

<1 %

23 Rob Simm, Mike Bacon. "References", Cambridge University Press (CUP), 2014

Publication

<1 %

Exclude quotes Off

Exclude matches Off

Exclude bibliography Off

Anisotropic properties identification of Naintupo Formation, Tabul Formation and Tarakan Formation (Tarakan Sub-Basin) using anisotropic parameters determination method from P-wave seismic diffraction

GRADEMARK REPORT

FINAL GRADE

GENERAL COMMENTS

/100

PAGE 1

PAGE 2

PAGE 3

PAGE 4

PAGE 5

PAGE 6

PAGE 7

PAGE 8

PAGE 9

PAGE 10

PAGE 11
